Thermo-Hydraulic Performance of Tubular Heat Exchanger with Opposite-Oriented Trapezoidal Wing Perforated Baffle Plate

Md. Atiqur Rahman*, S. M. Mozammil Hasnain, Rustem Zairov

Abstract: A detailed experimental study explored a new axial heat exchanger with swirling air over heated tubes. This heat exchanger features circular baffle plates with perforations and trapezoidal air deflectors at different angles. The tubes are aligned parallel to the airflow, and the deflectors create intense air turbulence, which improves heat transfer. The heat flux on the tubes is kept constant, and each baffle plate has eight deflectors positioned in reverse to induce swirling air within a circular duct that contains the hot water tubes. The baffle plates are spaced with varying pitch ratios, and the Reynolds number ranges from 16,000 to 30,000. The study found that the heat exchanger's performance highly depends on the pitch ratio and deflector angle, with the highest thermal enhancement factor (TEF) of 2.48 achieved at a 30° deflector angle and a pitch ratio of 1.2. These findings highlight the importance of optimizing design parameters to improve heat exchanger performance, offering valuable insights for better thermal management in industrial and environmental applications.

Keywords: deflector inclination angle; discontinuous swirl flow; flow recirculation; relative flow resistance; trapezoidal deflector; thermo-fluid performance

1 INTRODUCTION

Swirl flow is fluid motion along a helical or spiral path, where the particles possess tangential and axial velocity components. The resulting flow is called a helical/swirl when the fluid flows through a confined path, as in a shell or duct, either through suction or a forced flow generator [1].

Swirl flow is vital in various engineering and industrial applications for several reasons [2]:

1) Enhanced Mixing: Swirl flow enhances mixing efficiency by inducing tangential velocity components and axial flow. This is crucial in applications such as chemical reactors, where uniform mixing of reactants is essential for reaction efficiency.
2) Heat Transfer (HT) Improvement: In heat exchangers (HX) and cooling systems, swirl flow promotes better HT by creating turbulence and increasing the contact surface area between the air and the HT surface.
3) Reduction of Dead Zones: Swirl flow helps reduce stagnant or dead zones in fluid systems by imparting rotational motion. This is advantageous in preventing sedimentation or buildup of contaminants in pipelines or tanks.
4) Control of Flow Separation: In aerodynamics and fluid dynamics, swirl flow can help control flow separation over surfaces, which is crucial for maintaining aerodynamic efficiency and reducing drag in aircraft wings, turbines, and other applications.
5) Enhanced Combustion: In combustion chambers, swirl flow can improve combustion efficiency by ensuring better fuel-air mixing, leading to cleaner and more efficient combustion processes.
6) Vortex Formation: Swirl flow often leads to stable vortex structures, which can be utilized beneficially in various applications, such as vortex tubes for separating components of gas mixtures or cyclone separators for particle separation.

7) Energy Efficiency: By enhancing mixing and reducing flow losses, swirl flow contributes to overall energy efficiency in fluid systems, whether in industrial processes, HVAC systems, or environmental engineering applications.

Swirl flow in a confined path is generated using swirl generators. Swirl generators effectively enhance HT between the fluid and surfaces within the HX. These generators generate vortices or eddies that intensify fluid mixing, reducing boundary layer width and improving the convective heat transfer coefficient (h_m). Additionally, using swirl producers helps eliminate stagnant regions in the baffle spacing, ensuring an even heat distribution. Furthermore, these devices can regulate flow distribution, preventing fluid clogging or dead zone formation and ultimately enhancing the HX's overall efficiency (η) [3].

There are several ways to generate swirl flow characterized into three categories [4]:

- Use of fins or adjustable propellers tangentially deflecting the axial flow. Because of its simplicity, this device is generally used in industrial systems, particularly gas turbines. However, this type of device introduces significant head losses, and the swirl intensity is limited (design of fins) [5].
- Rotating mechanical devices generate a rotational movement of the fluid passing between them [6].
- Tangential injection of part or all fluid quantity into a main duct. The intensity of the swirl is then determined by the ratio between the flow injected tangentially and that injected axially [7, 8].

Swirl flows are highly valued for effectively mixing fluids and extending residence times, facilitating complete reactions. They are extensively employed in diverse engineering applications, including cyclone separators, separation processes, combustion chambers, turbo machinery, solar applications, heat exchangers, bubble

generators, electronics cooling, and environmental pollution mitigation systems [9].

There are two types of swirl generators: decaying and non-decaying. Decaying swirl generators [10, 11] create swirling or vortex-like motion that diminishes over time due to viscosity, friction, or turbulence, while non-decaying swirl generators sustain continuous swirling motion throughout the flow.

Recently, devices that create swirl have gained widespread use to enhance heat management across various industries. This adoption is due to their cost-effectiveness and straightforward installation procedures. The swirling patterns, known as vortices, are classified based on the orientation of their rotational axis [12]. Longitudinal vortices rotate perpendicular to the flow direction, whereas transverse vortices spin parallel. Creating these vortex structures has significantly enhanced heat transfer efficiency by optimizing flow characteristics within the stream [13, 14]. However, incorporating fins increases the system's flow resistance and friction losses, necessitating higher pumping power [15].

Many studies have focused on methods of generating swirls in the confined space. Inclined ribs, arc ribs, turbulators, twisted tape, guide vanes, blades, etc., generally do this despite the notable thermal enhancements resulting from implementing swirl generators; a significant Δp ensued, rendering the aforementioned thermal systems ineffective. Researchers have focussed on perforation as an alternate option, significantly reducing Δp and enhancing the thermal enhancement factor ($TEF = j/j_0/(f/f_0)^{1/3}$).

Perforations create openings or passages in a material, allowing for better airflow, heat dissipation, and improved thermal efficiency. Some key points highlighting the importance of perforation in heat transfer include [16]:

1) Improved Ventilation: Perforations enhance airflow through materials, which is crucial for efficient heat transfer by facilitating the removal of heat and preventing overheating.
2) Enhanced Surface Area: Perforations increase the material's surface area, promoting quicker heat dissipation and more effective thermal energy transfer.
3) Reduced Thermal Resistance: Perforations decrease thermal resistance by facilitating heat transfer across surfaces, allowing for faster cooling or heating depending on the application.
4) Improved Heat Dissipation: In applications requiring efficient heat dissipation, such as electronic devices or power systems, perforations aid in removing excess heat by promoting airflow through the material.
5) Customization and Flexibility: Perforations can be customized in various shapes and sizes to meet specific heat transfer needs. This flexibility enables optimization of heat transfer performance across different applications.

Researchers have explored modifying fins and baffles through openings and cavities to increase surface area and integrating slots and grooves to enhance fluid mixing and heat transfer efficiency. A few of the notable works have been discussed below.

Wang et al. [17] conducted experimental and numerical investigations on HT and friction (f) characteristics of vortex generators (VGs) using various hole shapes, including circular, equilateral triangle, square, rectangular, and rhombus holes. The study varied the pitch ratio (PR) from 1.63 to 4.89 while maintaining an angle of attack (α) of 45°. A comparison between planar VGs and VGs with drilled holes revealed that circular holes enhanced local heat dissipation by improving jet flow and promoting fluid rotation, which is particularly beneficial in recirculation zones. In contrast, hole shapes with sharp corners did not contribute positively to heat dissipation. A maximum TEF of 1.14 for Case A (circular holes) at Reynolds number (Re) = 9090 was noted.

In a separate study, Wang et al. [18] investigated the application of perforated VGs on mini-channel HX walls, an area with limited research. This study examined the influence of VG placement, PR, hole diameter, and VG configuration on the TEF of the HX. Results indicated that VG placement affects downstream vortex structures, where larger opening areas can suppress vortices or cause certain structures to vanish, potentially compromising HT performance. Optimal HT was observed at specific PR, highlighting the critical role of hole placement. Ajarostaghi et al. [19] introduced an innovative turbulator, showing an increase in Nusselt number (Nu) with the number of blades.

Mousavi et al. [20] numerically investigated the effects of incorporating a novel curved turbulator to enhance HT within a pipe. This turbulator includes multiple rows of flow directors designed to induce turbulent swirl flows. The study analyzed five geometric parameters—curvature angle, flow director diameter, cone angle, nozzle outlet diameter, and number of flow director rows—across the Re range of 10,000 - 35,000. The research findings indicate that the outlet diameter of the conical nozzle has minimal impact on thermal performance. Additionally, the TEF and overall heat transfer coefficient (U) improve as the number of flow director rows increases. Higher curvature angles lead to more pronounced secondary flows, resulting in higher average Nu. However, the curved turbulator configuration exhibits lower TPF than its uncurved counterpart due to significant Δp.

In their study, Wang et al. [21] investigated the effect of rotational motion on HT and fluid dynamics in a circular duct, incorporating a nozzle (conical) at the outlet. The researchers conducted experiments using a 1200 mm long pipe with an 80 mm diameter. They examined 3 different nozzle ratios (0.5 - 0.75) and tested seven distinct blade swirl generators under varied flow conditions. For the solid pipe experiments, flow Re ranged from 42,000 to 170,000. In contrast, the porous pipe experiments covered flow Re between 70,000 and 130,000, with BR varying between 0.002 and 0.050. The result indicated valuable information about h_m, overall Δp, and the characteristics of swirling flow, highlighting crucial phenomena, such as vortices forming along the pipe's central axis.

Hussein and Hameed [22] conducted an experimental study to assess the effectiveness of a double-pipe HX in facilitating HT between air and water. Segmental baffle plates (SBP) featuring semi-circular holes were employed to

enhance HT. The edges of these semi-circular holes were modified to act like fins. Air served as the HT fluid in the annular region between the shell and tube of the HX, while water flowed through the tube. The airflow Re ranged from 2700 to 4000 across seven distinct conditions, while the water flow maintained a constant Re of 34159. Three sizes of semi-circular holes (30 mm, 25 mm, and 20 mm in diameter) were investigated to evaluate their impact on the TPF(Thermal performance factor) of HX. Assessment criteria included Nu, U, and TPF, and configurations with and without baffles were compared. Results indicated significant enhancement in TPF with baffles, increasing the average h_m by 29.7%, 62%, and 80.6% for hole diameters of 30 mm, 25 mm, and 20 mm, respectively, with the best TPF achieved using baffles with 20 mm diameter holes.

Hassan et al. [23] investigated the impact of hole number and shape on the TEF of both solid and perforated conical rings. The study examined convergent and divergent ring configurations, each with 25 mm and 50 mm end diameters, resulting in a diameter ratio 0.5. The rings had a consistent thickness of 2 mm and a length of 60 mm. The distance between consecutive rings was fixed at 120 mm to maintain a pitch-to-diameter ratio (p/d) 1.875. A constant heat flux of 3000 W/m² was applied to the outer tube, while the Re varied from 6000 to 26000. Results showed that solid divergent rings achieved higher Nu, reaching 360.2 at Re = 26000. However, this configuration also exhibited the highest f, peaking at 5.04 at Re = 6000; perforating the rings with circular, square, or equilateral triangular holes reduced both the Nu and f, thereby enhancing TEF, especially with more holes. Circular holes demonstrated the highest TEF, while triangular holes showed the lowest. For solid divergent rings at Re = 6000, a maximum TEF of 1.1 was achieved. In contrast, circularly perforated rings achieved a TEF of 1.06 with lower pumping power requirements, showcasing improved thermal performance while maintaining efficiency.

A unique type of heat exchanger, referred to as an axial flow tubular heat exchanger, was developed by Rahman and Dhiman [2, 24, 25]. The purpose was to enhance the HT by creating a swirl airflow path across the tube bundle in a tubular HX. Perforated circular baffle plates with trapezoidal air deflectors(inclined at various angles) were used to generate swirl flow. Each plate has four deflectors arranged clockwise at identical angles, creating a swirling flow as air enters the HX. However, the tube configuration remained unchanged, maintaining a consistent heat flow.

Consequently, the swirling motion increased turbulence in the air, improving HT. The study was conducted by varying the baffle spacing under the Re range of 16000 to 28000. The influence of PR and α on the h_m and f of the HX was investigated. The result revealed that an HX with a deflector angle of 50° and a Pitch ratio (l/D) of 1.4 displayed an augmentation of 3.75 in TPF compared to others. This work was further extended by Rahman [26], who used an oriented trapezoidal deflector and found an increase in TEF of 2% compared to Rahman and Dhiman[24].

Rahman, M. A. [26, 27] further explored the consequence of rectangular punched holes with one or two flow deflectors. The influence of deflector orientation on heat transfer and fluidic performance was estimated through experiments. When using one deflector, a surge of 41.49% was seen in TPF. Employing two flow deflectors of opposing orientations decreased TEF by 0.19 times compared to an HX with an SBP. The results indicated that the opposite-oriented deflectors achieved a higher HT rate than inline ones, although this advantage came with higher Δp losses. Rahman [28, 29] further directed his work to see the effect of multiple rectangular deflectors' orientations (inline shutter type and opposite-oriented). The result indicated that the shutter type shows a higher TEF; however, the opposite orientation of the deflector shows a higher h_m and higher Δp. Going further, Rahman studied different deflector geometries, such as triangular [29] and sawteeth [30]. Upon changing the shape of the baffle plate from circular to conical [31-33], Rahman achieved a higher hm value nearly 1.5 times compared to the circular baffle plate at the expense of Δp.

Based on the analysis of the gathered data, the following insights have been observed regarding the HT properties of non-decaying swirl flow:

1) The Nu for swirl flow exceeded that of axial flow. This enhancement is due to higher local velocities, increased turbulence, and buoyant forces caused by the flow's curvature and centrifugal effects.
2) Significant Δp occur because baffles obstruct fluid flow, causing flow separation near the edges of the baffles. Consequently, greater pumping power is often required to compensate for the increased Δp while maintaining the same heat load.
3) A smaller pitch ratio typically results in higher heat transfer rates and greater Δp.

Additionally, swirl flow facilitates the HX's compaction, ultimately improving space efficiency. Swirlers can also aid in eliminating stagnation zones by promoting a more uniform temperature distribution over the tube surface, which proves essential in applications where a uniform temperature profile is critical, such as thermal processing or heating/cooling scenarios.

The recent work on swirl generation mentioned above in the literature indicates that the performance of an HX is not solely dependent on the Re/velocity/mass flow rate of the working fluid but is sensitive to the direction of flow (parallel/counter flow) but also a type of flow (axial/radial/swirl). Among these, swirl flow gives a maximum TEF value. Nonetheless, there is limited research on the thermal-fluid properties of HX featuring baffle plates as turbulators. It is also noted that the TEF is sensitive to the geometry of the swirler, as shown by Rahman [32-43]. Only a handful of geometry has been studied, requiring further exploration. Furthermore, using air as a working fluid has been insufficiently studied despite its numerous advantages, such as ease of disturbance introduction and lower fouling resistance than other liquids. Although air allows for better flow control due to its non-sticky nature, its hydrodynamic and thermal boundary layers resemble those of other liquids.

This study aims to develop and experiment with a novel swirl generator which employs trapezoidal deflectors (TDBP) positioned opposite each other on the baffle plates.

Through the experimental evaluation processes, the following objectives were planned:

- To develop setup and fabricate swirl-inducing perforated baffle plate designs with flow deflectors and its validation with the reported work.
- To investigate the effect of deflector's α on heat transfer for various Re.
- To investigate the baffle plate spacing (PR) effect on HT for various Re.
- To investigate how the Δp and f have been affected by varying the Re and PR of the HX.
- To estimate TEF of the HX by varying PR, α, Re based on j, f, Δp.

The parameter range is as follows:

- PR (l/D): 0.6, 0.8, 1, 1.2.
- α (inclination angle): 30°, 40°, 50°.
- Re (Reynolds number): 15,000 to 30,000.

The resultant Nu, f values are compared with those obtained from HX without a baffle plate working under similar operation parameters.

2 METHODOLOGY
2.1 Experimental Setup with HX Details

The experiment employs a variety of equipment, including the air intake unit, HX, pressure and temperature gauges, a water-circulating loop, and a data acquisition system. Detailed information about the equipment can be seen in references 3, 24, and 25. Three pressure ports are generated on both the inlet and exit of the HX to obtain the Δp. Ten RTD thermocouple probes are pasted on the tube surface carrying hot water to acquire surface temperature (using DAQ assistant NI-9213 thermocouple modules), and two additional thermocouples are used to acquire air temperature as it arrives and departs the HX. The velocity of air is calculated using the pitot tube. The 8 kW variac electrical heating element with thermostat (SSU 0-300 °C) controlled ensures a constant temperature of 60 °C for the heated water. A pump and Rotameter (LZS-25) control the hot water flow rate. The airflow rate can be adjusted while keeping the flow rate (water) constant during the experiment.

Table 1 Testing conditions used in experiments [32, 33]

Air-inlet temperature, °C	32.5 ± 0.5
Air-inlet velocity, m/s	7 - 10
Water-inlet temperature, °C	60 - 65
Water mass flow rate, kg/s	0.06

The experimentation conditions are outlined in Tab. 1, with the precision of the instruments is evaluated using the root mean square method, with precision in temperature measurement of ± 0.5, Δp of ± 0.1, and flow rate of ± 0.006. The approximate highest level of uncertainty connected with the $Re = \pm 3.25$, $v = \pm 5$, $f = \pm 5.34$, and $Q = \pm 5\%$.

The test section revealed in Fig. 1 is an acrylic duct with a length of 60 cm, a width of 19 cm, and a thickness of 0.5 cm, with a thermal conductivity (k_p) of 0.2. Parallel to the duct are copper tubes composed of Copper (C12200), which have a $k_t = 300$ (W/mK). The tubes possess an inner width of

8 mm with a thickness of 1mm, carrying hot water supplied by the distributor. They are supported by innovative baffles [32-40].
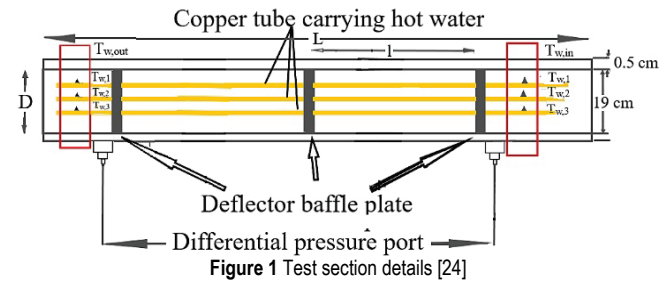

Figure 1 Test section details [24]

In contrast, the fluid on the other side of the duct is air drawn in from the surroundings, as the primary focus of this study is on air. Two groups of thermocouples are utilized to acquire the surface temperature of the copper tubes carrying the hot fluid: $T_{w, in}$, and $T_{w, out}$. Each group contains 5 thermocouples (t_{w1}-t_{w5}), one devoted to each tube. The arrangement of these thermocouples for capturing the temperature at the inlet and outlet of the copper tubes is illustrated by Rahman [32, 33]. Moreover, additional thermocouples ($T_{a, in}$ and $T_{a, out}$) are employed to record the air temperature as it passes through the test section.
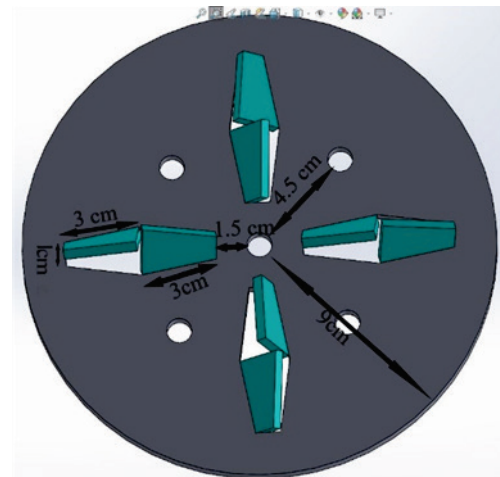

Figure 2 CAD model of Trapazoidal deflector baffle plate

The diagram in Fig. 2 illustrates the latest Trapezoidal Deflector Baffle Plate (TDBP) developed. It features a single central tube encircled by four supplementary tubes organized in a circular formation. These tubes are arranged 4.5 cm from the centre at an angle of 60° from each other. The TDBP has four openings to enable airflow into the ducts. The trapezoidal holes have been designed with $1d$ and $2d$ dimensions for the parallel sides and a side of $3d$, where d represents the tube diameter (1 cm). Two identically sized trapezoidal deflectors have been pasted in reverse at a prearranged angle alongside the baffle plate (as shown in Fig. 3a). The deflector arrangement converts airflow from axial to swirl patterns. The deflector's presence initiates swirl motion in the axial air stream, transforming the airflow into a well-defined swirling pattern as it passes through the tube bundles. The angle α strengthens the axial flow and converts it into plug flow.
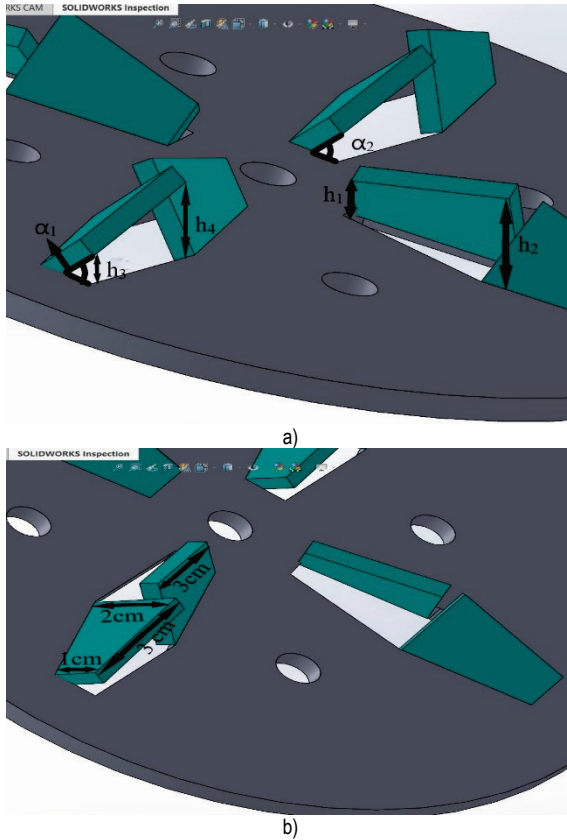
a)

b)

Figure 3 a) Baffle plate detail and b) deflector detail

Consequently, opposite swirl streams are generated in the baffle spacing, preventing the formation of stagnant zone. The swirling motion increases Δp and augments HT. The baffle plates spacing, known as the pitch of the baffle plate, is crutial in formation of vortices, recirculation, and turbulence within the baffle spacing. This study evaluated their impact by examining PR values of 0.6, 0.8, 1, and 1.2. As a result, turbulence and vortices are generated within the duct due to the rotational air structures, which constantly clean the tube wall and manipulate the thermal boundary layer. The research investigates three different angles: α = 30°, 40°, and 50°. This setup creates an opening similar to a vent, allowing air circulation and serving as the flow area. The deflectors are located 15 mm from the center. All deflectors have the constant height ratio (h_1/h_2 and h_3/h_4 = 0.5) irrespective of the α, as shown in Fig. 3b

2.2 Design Constraint and Data Reduction

Pitch ratio [24-28] is estimated as

$$PR = \frac{l}{D} \tag{1}$$

Blockage ratio [30-32] is estimated using

$$BR = \frac{U}{S} \tag{2}$$

Where U is the cross-sectional area of the baffle plate (4 times the cross-sectional area of the rectangular opening) and S is the cross-sectional area of the baffle plate.

This paper examined the impact of TDBP in a circular channel on thermo-hydraulic performance, with a fixed BR value of 0.7, under different Re conditions. To gather data, multiple tests were conducted on the channel using various baffle plates with different α (30°, 40°, and 50°). A separate experiment was also carried out on a channel within the same Re range without a baffle. The obtained results were evaluated to determine the effects of PR and α on the heat exchanger's thermo-hydraulic efficiency.

Ranman's [24] method calculates the mean convection heat transfer coefficient ($h_{c,m}$ in W/m²K).

$$Re = \frac{\rho \cdot v \cdot D_h}{\mu} \tag{3}$$

Where v represents the average speed in meters per second and D_h as the hydraulic diameter of the circular tube in meters. In this situation, we can compute the thermal properties of air, such as ρ (density in kg/m³) and μ (dynamic viscosity coefficient in kg/m-s), by using the average temperature values of the air entering and leaving the system.

$$v = \sqrt{\frac{2\Delta p_o}{\rho}} \tag{4}$$

$$h_m = \frac{Q}{A_p \cdot \Delta t_{lm}} \tag{5}$$

In the given scenario, Q represents the rate at which heat is transferred from the air side, measured in Watts. The A_p symbolizes the heat transfer area on the copper tube, which is expressed in square meters. ΔP_o indicates the pressure drop at the orifice plate, measured in Pascals, and Δt_{lm} refers to the logarithmic mean temperature difference between the air and the copper tube's wall. HT rate is calculated as.

$$Q = C_p \cdot \rho \cdot v \cdot A_c \cdot (T_{a,\,out} - T_{a,\,in}) \tag{6}$$

A_c is annulus crossectional area, calculated as

$$A_c = \frac{\pi}{4} \cdot (D - D_e) \tag{7}$$

Where: D_e is the equivalent diameter of the HX; $T_{a,\,in}$ and $T_{a,\,out}$ average air temperature at inlet and outlet, respectively, whereas Δt_{lm} is LMTD for parallel flow given as

$$\Delta t_{lm} = \frac{(T_{w,\,in} - T_{a,\,in}) - (T_{w,\,out} - T_{a,\,out})}{\dfrac{\ln(T_{w,\,in} - T_{a,\,in})}{(T_{w,\,out} - T_{a,\,out})}} \tag{8}$$

when $T_{w,\,in}$ and $T_{w,\,out}$ are the average copper surface temperature at inlet and exit, respectively, determined as

follows:

$$T_{w,\,in} = \left(\cfrac{\sum\limits_{1}^{5} t_{w,\,i}\,A_i}{A_p}\right)_{in} , \quad T_{w,\,out} = \left(\cfrac{\sum\limits_{1}^{5} t_{w,\,i}\,A_i}{A_p}\right)_{out} \qquad (9)$$

The heating module contains five temperature junctions, indicated as i, on the copper pipe. These junctions are positioned at the entry and exit points of the experimental segment, aligning with the airflow. A_i corresponds to the surface area responsible for heat transfer. The average Nusselt number (Nu) and friction factor (f) are employed to express the flow and thermal characteristics of the duct.

$$Nu = \frac{h_{c,\,m} D_h}{\lambda} \qquad (10)$$

$$f = \frac{2\Delta P \cdot D}{\rho \cdot v^2 \cdot L} \qquad (11)$$

Δp is the pressure drop in the HX.

From Eqs. (5) and (6) follows

$$h_m = \frac{C_p \cdot \rho \cdot v \cdot A_c \cdot (T_{a,\,out} - T_{a,\,in})}{A_p \cdot \Delta t_{lm}} \qquad (12)$$

Reative dimensionless quantities such as thermal transfer enhancement (j/j_0), relative flow obstruction (f/f_0), and a benchmark $TEF = (j/j_0)/(f/f_0)^{(1/3)}$ were utilized. The j and f values of an HX with a Baffle plate, while f_0 and j_0 are for HX without a baffle plate [38-43].

2.3 Validation

To assess the precision of the experiment, the obtained Nu and f are compared with values derived from standard correlations. Nu is calculated using the Gnielinski, and Dittus equations, while the Colebrook-White and Blasius correlations are employed for f. The comparison reveals the following mean deviations from experimental values: −9.054% for Gnielinski, +8.195% for Dittus and Boelter, +0.73% for Blasius and −0.649% for Colebrook-White [32].

3 RESULTS AND DISCUSSION
3.1 HT Augmentation

Enhancing HT can be achieved by installing a deflector baffle, which induces turbulent flow and disrupts thermal boundary layer formation for the experimental Re range.

Fig. 4 depicts the variation of the relative colburn factor (j/j_0) as a function of Re. Initially, there is an increase in j/j_0 until it reaches its peak value, followed by a gradual decline with a rise in Re. This pattern is observed consistently for all tested samples of the turbulent deflector baffle plate (TDBP). It also shows that increasing α value leads to a decline in j/j_0.

In turbulent flow, the energy accompanying the chaotic fluid movements or eddies is distributed throughout the fluid due to molecular interaction, generating multiple convective cells that facilitate faster HT than laminar flow. The transport of energy through cell interaction is effective across a large area, expediting the diffusion process. The movement of these eddies generates areas of varying Δp, replenishing the energy required for convection and accelerating the HT rate. Therefore, turbulent flow promotes HT by enhancing convection and diffusion. Fascinatingly, as α declines, so does the flow area in this scenario deflector now acting as nozzle; further increase in Re value makes flow unstable.
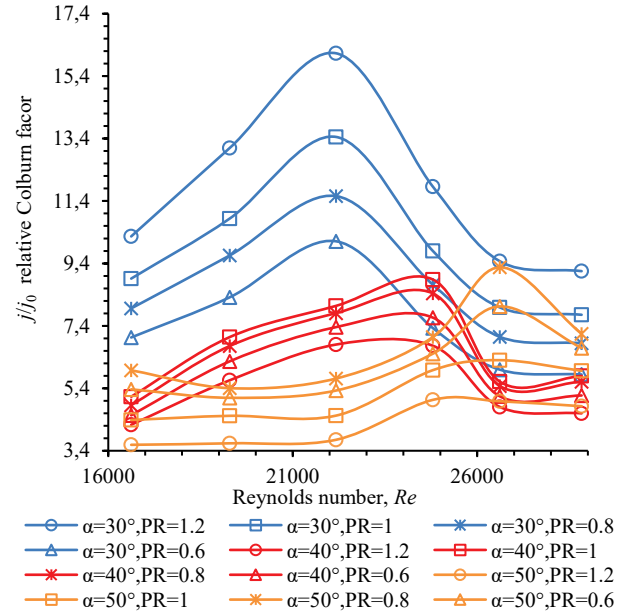

Figure 4 Heat transfer enhancement

For a deflector angle of 30°, the TDBP samples show the highest j/j_0 ratios compared to others. This indicates that a lower angle increases flow disruption and instability. When the deflector is angled towards the baffle plate, it narrows the flow area abruptly, boosting air velocity in the duct and creating a jet effect. This setup prevents boundary layer formation on the tube and wall, while the rotating fluid washes over the tube bundles, inducing a spiral flow that enhances mixing and HT.

Increased flow velocity improves the fluid's ability to clear the duct area, lowering dynamic air Δp near the walls of the duct and tube, enhancing heat transfer efficiency and raising Δp. The angle of the deflector significantly influences heat transfer rates: as the α declines, local air velocity and turbulence increase, leading to greater cavitation and enhanced air molecule interaction with the wall, which boosts heat transfer from the wall.

Research by Wang et al. [34] found that very close spacing between deflector baffles intensifies vortex interactions, causing them to break up and reduce heat transfer. Conversely, boundary layer separation occurs too early if the spacing is too broad, leading to higher pressure loss. Therefore, optimizing the spacing (PR) between

turbulent deflector baffle plates is crucial for maximizing heat transfer. Tab. 2 details the highest j/j_0 ratio for various Re, PR, and α.

Table 2 Maximum values

α	j/j_0			j/j_0		
	Max value			Max values		
	PR	j/j_0	Re	PR	Re	j/j_0
30	1.2	16.13	22200	0.6	29000	9.38
40	1	8.88	24800	0.6	29000	8.61
50	0.8	9.27	26600	0.6	29000	7.64

According to a study conducted by Wang et al. [34], smaller PR optimizes HT. This finding is sustained by the information provided in Tab. 2, which shows that the PR increases as the α increases.

The turbulence created in the baffle plate spacing affects the HT rate. When the PR is set at 1.2 and α is 30°, the average j/j_0 peaks at 16.13. On the other hand, for higher α values, the highest average j/j_0 is achieved at lower PR values such as 1 and 0.8. A smaller PR reduces the baffle spacing available for air and surface interaction. This promotes flow reversal and enhances the tube washing ability, resulting in better heat transfer performance ($h_{c, m}$).

Conversely, heat transfer diminishes as the PR increases due to a lower interface interaction between the fluids and wall, leading to lower $h_{c, m}$ values and slower heat transfer rates. Additionally, when the baffle spacing increases, the ΔT between the tube surface and the surrounding air decreases, resulting in a decline of HT. A decline in thermal contact (surface and air) causes this.

3.2 Relative Flow Resistance and Thermo-Fluid Performance

The data in Fig. 5 illustrates the relationship amongst f/f_0 and Re. All TDBP models exhibit a comparable trend, with f/f_0 starting low at lower Re and rising until reaching a peak. The maximum f/f_0 value was noted at $\alpha = 30°$, which declines with increasing α and PR. Consequently, at $\alpha = 30°$, it shows maximum HT and f losses, particularly at PR of 0.6. As α increased beyond 30°, the occurrence of blockages decreased, leading to reduced turbulent flow and limited eddies that typically cause pressure fluctuations along the inner side of the duct.

Previous research indicates that regions with higher turbulence, velocity, and extended fluid-surface interactions experience increased Δp. Consequently, it is anticipated that Δp will follow the sequence of $\alpha = 30°$, 40°, and 50°. With smaller PR, lower α values lead to higher average f/f_0, with a peak of 9.38 at $\alpha = 30°$ and PR = 0.6. The addition of deflectors can increase Δp by disrupting the fluid's kinetic energy as it flows along the HX. The deflector having the smallest α generates a prominent swirling motion, resulting in substantial rotational interaction amongst the secondary flow and the wall. This interaction creates significant turbulence, causing a high Δp with elevated f.
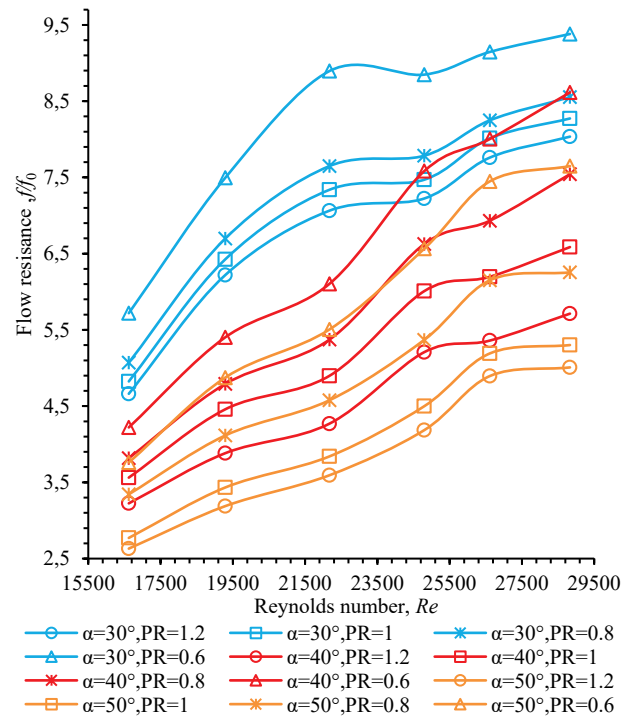
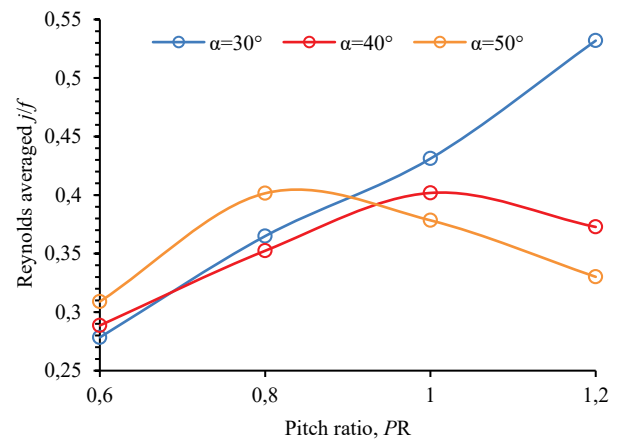**Figure 5** Flow resistance vs Re

Figure 6 Area goodness factor vs PR

The term Area goodness factors defy the compactness of HX. Fig. 6 shows Reynonald's average j/f, which shows that higher PR works best for a given range of Re, i.e., 1.2, whose value reduces with a rise in α. Furthermore, the TEF of the heat exchanges has been analyzed and plotted in Fig. 7, which shows a similar trend as Fig. 5, displaying higher TEF values at lower α. The maximum TEF is seen at α of 30° because of immense turbulence due to swirl flow generated by low α and multiple baffles along the flow. This is because increasing PR increases the area for airflow, reducing Δp and lower velocity. The maximum TEF of 2.48 is seen at PR of 1.2 and an α of 30°.
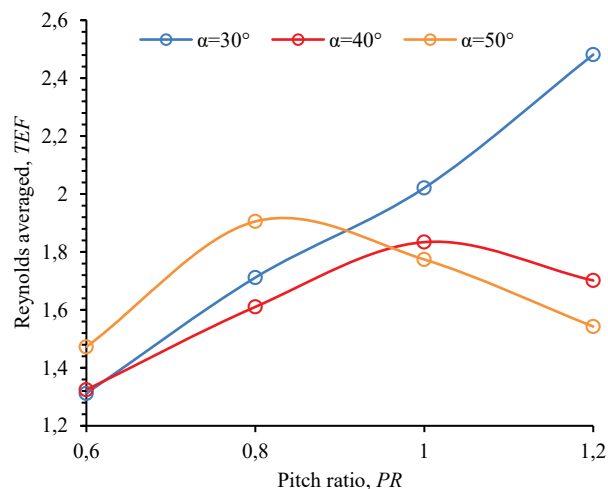
Figure 7 Thermal enhancement factor vs PR

4 CONCLUSIONS

The analysis of TDBP samples showed that increasing the duct α led to higher flow velocities, with increments of 29.6%, 21.7%, and 14.2% for α values of 30°, 40°, and 50°, respectively, in comparison to ducts without baffle plates. The HX gives optimal value for smaller α value and higher PR, with the TEF peaking at 2.48 for $\alpha = 30°$. Δp was greatest at smaller α values, showing reductions of 31.37%, 22.94%, and 17.31% for $\alpha = 30°$, 40°, and 50°, respectively. The TDBP worked efficiently with Re below 25,000, providing good HT and f properties, although these diminished at higher Re. The impact of PR was minimal with air as the working fluid, suggesting that future studies should explore high-density fluids like slurry, water or oil. Different deflector arrangements should also be investigated to enhance swirl flow and TEF. The current study used a fixed baffle ratio (BR) of 0.7, which could be increased to lower Δp, and achieved a maximum velocity of 13 m/s, which could be further increased. The research focused on three baffle plates with four different PR values; exploring additional baffles and PR values and a wider range of α values is recommended. Finally, while the study used non-metallic baffle plates, future research should incorporate metallic plates to contribute actively to HT.

5 REFERENCES

[1] Rahman, M. A. & Dhiman, S. K. (2024). Study of Flow and Heat Transfer in Swirled Tubular Recuperator. http://hdl.handle.net/10603/576426

[2] Rahman, M. A. & Hasnain, S. M. M. (2024). Performance Improvement of Heat Exchanger with Perforated/Non Perforated Flow Modulator Producing Continous/Discontinous Swirl Flow. *Heat transfer*. https://doi.org/10.1002/htj.23135

[3] Rahman, M. A. & Dhiman, S. K. (2023). Performance evaluation of turbulent circular heat exchanger with a novel flow deflector-type baffle plate. *Journal of Engineering Research*, 100105. https://doi.org/10.1016/j.jer.2023.100105

[4] Boushaki, T. (2019). Introductory Chapter: Swirling Flows and Flames. IntechOpen. https://doi.org/10.5772/intechopen.86495

[5] Iyogun, C. O., Birouk, M. & Kozinski, J. A. (2011). Experimental investigation of the effect of fuel nozzle geometry on the stability of a swirling non-premixed methane flame. *Fuel, 90*(4), 1416-1423. https://doi.org/10.1016/j.fuel.2010.12.033

[6] Schmittel, P., Günther, B., Lenze, B., Leuckel, W. & Bockhorn, H. (2000). Turbulent swirling flames: Experimental investigation of the flow field and formation of nitrogen oxide. *Proceedings of the Combustion Institute, 28*(1), 303-309. https://doi.org/10.1016/S0082-0784(00)80224-6

[7] Boushaki, T., Sautet, J. C. & Labegorre, B. (2009). Control of flames by tangential jet actuators in oxy-fuel burners. *Combustion and flame, 156*(11), 2043-2055. https://doi.org/10.1016/j.combustflame.2009.06.013

[8] Elbaz, A. M. & Roberts, W. L. (2016). Investigation of the effects of quarl and initial conditions on swirling non-premixed methane flames: Flow field, temperature, and species distributions. *Fuel*, 169, 120-134. https://doi.org/10.1016/j.fuel.2015.12.015

[9] Rahman, Md. A., Hasnain, S. M. M., Pandey, S., Tapalova, A., Akylbekov, N. & Zairov, R. (2024). Review on Nanofluids: Preparation, Properties, Stability, and Thermal Performance Augmentation in Heat Transfer Applications. *ACS Omega*. https://doi.org/10.1021/acsomega.4c03279

[10] Sarac, B. A. & Bali, T. (2007). An experimental study on heat transfer and pressure drop characteristics of decaying swirl flow through a circular pipe with a vortex generator. *Experimental Thermal and Fluid Science, 32*(1), 158-165. https://doi.org/10.1016/j.expthermflusci.2007.03.002

[11] Jafari, M., Farhadi, M. & Sedighi, K. (2017). An experimental study on the effects of a new swirl generator on thermal performance of a circular tube. *International Communications in Heat and Mass Transfer*, 87, 277-287. https://doi.org/10.1016/j.icheatmasstransfer.2017.07.016

[12] Rahman, M. A., Hasnain, S. M. M. & Zairov, R. (2024). Assessment of improving heat exchanger thermal performance through implementation of swirling flow technology. *International Journal of Thermofluids*, 22, 100689. https://doi.org/10.1016/j.ijft.2024.100689

[13] Nair, S. R., Oon, C. S., Tan, M. K., Mahalingam, S., Manap, A. & Kazi, S. N. (2022). Investigation of heat transfer performance within annular geometries with swirl-inducing fins using clove-treated graphene nanoplatelet colloidal suspension. *Journal of Thermal Analysis and Calorimetry, 147*(2), 14873-14890. https://doi.org/10.1007/s10973-022-11733-6

[14] He, Y. L. & Zhang, Y. (2012), Advances and Outlooks of Heat Transfer Enhancement by Longitudinal Vortex Generators, *Advances in Heat Transfer*, 44, 119-185. https://doi.org/10.1016/B978-0-12-396529-5.00002-0

[15] Suja, S. B., Islam, M. & Ahmed, Z. U. (2023). Swirling jet impingements for thermal management of high concentrator solar cells using nanofluids. *International Journal of Thermofluids*, 19, 100387. https://doi.org/10.1016/j.ijft.2023.100387

[16] Rahman, Md. A. & Hasnain, S. M. M. (2024). Performance improvement of heat exchanger with perforated/non perforated flow modulator producing continous/discontinous swirl flow: A comprehensive review. *Heat transfer*. Vol. ahead-of-print No. ahead-of-print. https://doi.org/10.1002/htj.23135

[17] Wang, J., Fu, T., Zeng, L., Lien, F. S., Wang, H. & Deng, X. (2022). A Comparative study on thermo-hydraulic performance in a tube with different punched winglets, *International Journal of Thermal Sciences*, 181, 107772. https://doi.org/10.1016/j.ijthermalsci.2022.107772

[18] Wang, J., Zeng, L., Fu, T., Yu, S. & He, Y. (2024). Effects of the position and perforation parameters of the delta winglet vortex generators on flow and heat transfer in mini channels. *International Journal of Thermal Sciences*, 198, 108878. https://doi.org/10.1016/j.ijthermalsci.2023.108878

[19] Ajarostaghi, M., Zaboli, S. S., Kiani, B. M., Saedodin, S., Karimi, N. & Javadi, H. (2022). Hydrogen preheating in a PEMFC system employing a heat exchanger equipped with an innovative turbulator. *International Journal of Hydrogen Energy,* 47(85), 36264-36282. https://doi.org/10.1016/j.ijhydene.2022.08.204

[20] Mousavi Ajarostaghi, S. S., Aghanezhad, M., Davudi, H. & Mohammadzadeh Amiri, M. (2021). Numerical evaluation of the heat transfer enhancement in a tube with a curved conical turbulator insert. *International Journal of Ambient Energy*, 43(1), 5218-5231. https://doi.org/10.1080/01430750.2021.1945490

[21] Wang, D., Khalatov, A., Shi-Ju, E. & Borisov, I. (2022). Swirl flow heat transfer and flow characteristics in a solid and permeable pipe with exit nozzle. *International Journal of Thermal Sciences*, 173, 107425. https://doi.org/10.1016/j.ijthermalsci.2021.107425

[22] Hussein, M. A. & Hameed, V. M. (2022), Experimental Investigation on the Effect of Semi-circular Perforated Baffles with Semi-circular Fins on Air–Water Double Pipe Heat Exchanger. *Arabian Journal for Science and Engineering, 47*, pp. 6115-6124. https://doi.org/10.1007/s13369-021-05869-0

[23] Hassan, A. Md., Al-Tohamy, A. H. & Kaood, A. (2022), Hydrothermal characteristics of turbulent flow in a tube with solid and perforated conical rings. *International Communications in Heat and Mass Transfer, 134*. https://doi.org/10.1016/j.icheatmasstransfer.2022.106000

[24] Rahman, M. A. & Dhiman, S. K. (2023). Investigations of the turbulent thermo-fluid performance in a circular heat exchanger with a novel flow deflector-type baffle plate. *Bulletin of the Polish Academy of Sciences Technical Sciences*. https://doi.org/10.24425/bpasts.2023.145939

[25] Rahman, M. A. & Dhiman, S. K. (2024). Investigations on thermo-fluid performance of a circular heat exchanger with a novel trapezoidal deflector-type baffle plate. *Thermal engineering*, 10, 1-13. https://doi.org/10.56304/S0040363624700292

[26] Rahman, M. A. (2024). Study the effect of axially perforated baffle plate with multiple opposite-oriented trapezoidal flow deflectors in an air–water tubular heat exchanger. *World Journal of Engineering*, Vol. ahead-of-print No. ahead-of-print. https://doi.org/10.1108/WJE-10-2023-0425

[27] Rahman, M. A. (2023). Experimental Investigations on Single-Phase Heat Transfer Enhancement in an Air-To-Water Heat Exchanger with Rectangular Perforated Flow Deflector Baffle Plate. *International Journal of Thermodynamics*, 1-9. https://doi.org/10.5541/ijot.1285385

[26] Rahman, M. A. (2023). Effectiveness of a tubular heat exchanger and a novel perforated rectangular flow-deflector type baffle plate with opposing orientation. *World Journal of Engineering*. https://doi.org/10.1108/WJE-06-2023-0233

[27] Rahman, M. A. (2024). Thermo-hydraulic effect of tubular heat exchanger fitted with Perforated baffle plate with rectangular shutter-type deflector, *Korean Chem. Eng. Res., 62*(2), 1-9. https://doi.org/10.9713/kcer.2024.62.2.1

[28] Rahman, M. A. (2024). Thermo-Fluid Performance Comparison of an Inline Perforated Baffle with Oppositely Oriented Rectangular-Wing Structure in Turbulent Heat Exchanger. *International Journal of Fluid Mechanics Research*, 51(1), 15-30. https://doi.org/10.1615/InterJFluidMechRes.2023051418

[29] Rahman, M. A. (2024). The effect of triangular shutter type flow deflector perforated baffle plate on the thermofluid performance of a heat exchanger. *Heat Transfer, 53*(2), 939-956. https://doi.org/10.1002/htj.22981

[30] Rahman, M. A. (2024). Thermal hydraulic performance of a tubular heat exchanger with inline perforated baffle with shutter type saw tooth turbulator. *Heat Transfer, 53*, 2234-2256. https://doi.org/10.1002/htj.23034

[31] Rahman, M. A. (2024). Thermo-Fluid Performance of a Heat Exchanger with a Novel Perforated Flow Deflector Type Conical Baffles. *Journal of thermal engineering, 10*(4), 868-879. https://doi.org/10.14744/thermal.0000846

[32] Rahman, M. A. (2024). The influence of geometrical and operational parameters on thermofluid performance of discontinuous colonial self-swirl-inducing baffle plate in a tubular heat exchanger. *Heat Transfer, 53*, 328-345. https://doi.org/10.1002/htj.22956

[33] Rahman, M. A. (2024). Thermal performance of tubular heat exchangers with the discontinuous swirl-inducing conical baffle with opposite-oriented flow deflectors. *Archives of Thermodynamics, 45*(2), 195-204. https://doi.org/10.24425/ather.2024.150865

[34] Wang, D., Khalatov, A., Shi-Ju, E. & Borisov, I. (2022). Swirl flow heat transfer and flow characteristics in a solid and permeable pipe with exit nozzle. *International Journal of Thermal Sciences,* 173, 107425. https://doi.org/10.1016/j.ijthermalsci.2021.107425

Author's contacts:

Md. Atiqur Rahman [a, b]
(Corresponding Author)
[a] Department of Mechanical Engineering,
Vignan's Foundation for Science, Technology & Research
(Deemed to be University),
Vadlamudi, Guntur-522213, Andhra Pradesh, India
rahman.md4u@gmail.com

[b] Department of Mechanical Engineering,
Birla Institute of Technology,
Mesra, Ranchi-835215, India

S. M. Mozammil Hasnain
Marwadi University Research Centre,
Department of Mechanical Engineering,
Faculty of Engineering & Technology,
Marwadi University,
Rajkot, Gujrat-360003, India

Rustem Zairov
Aleksander Butlerov Institute of Chemistry,
Kazan Federal University,
1/29 Lobachevskogo Str., Kazan 420008, Russian Federation